Renewable Energy 145 (2020) 1985–1991

Contents lists available at ScienceDirect

Renewable Energy

journal homepage: www.elsevier.com/locate/renene

Electron-mediated carbohydrate fuel cells: Characterizing the homogeneous viologen-mediated electron transfer rate of carbohydrate oxidation

Hilary Bingham [a], Dan Oliveira [a], Cassandra Larimer [a], Hayden Hedworth [a], Meisam Bahari [a], Gerald D. Watt [b], John N. Harb [a], Randy S. Lewis [a, *]

[a] Department of Chemical Engineering, Brigham Young University, Provo, UT, 84602, USA
[b] Department of Chemistry, Brigham Young University, Provo, UT, 84602, USA

ARTICLE INFO

Article history:
Received 12 November 2018
Received in revised form
11 June 2019
Accepted 15 July 2019
Available online 16 July 2019

Keywords:
Fuel cell
Viologen
Carbohydrate
Model
Homogeneous reaction

ABSTRACT

One area of exploration for renewable energy is the development of fuel cells, including carbohydrate fuel cells that can extract energy from carbohydrates. Viologen electron mediators have been shown to enhance energy extraction and improve carbohydrate conversion efficiencies, although the limiting step appears to be the homogeneous rate at which electrons are first transferred from the carbohydrate to the viologen. In this work, electron transfer rates for various monosaccharides in the presence of methyl viologen were studied in the absence of a fuel cell to isolate the homogeneous rate. Using glucose as the model carbohydrate, a rigorous mechanistic model of the homogeneous electron transfer rate was developed and showed a first-order dependence on OH^- concentration, a first-order dependence on carbohydrate concentration, a zero-order dependence when the methyl viologen concentration was $\gg$ 0.4 mM, and an increasing rate with incubation time when glucose was incubated in a buffer solution prior to exposure to methyl viologen. The incubation effect had a strong dependence on pH and was consistent with interconversion between glucose and fructose. The mechanistic model, which agreed well with experimental data, can be useful for identifying process improvements to carbohydrate fuel cells, especially when the homogenous rate is a limiting step.

1. Introduction

Energy use continues to increase and significant efforts are being expended to provide more renewable energy. Nearly 90% of energy consumed comes from nonrenewable resources such as petroleum, coal, natural gas, and nuclear, with the remainder from renewable resources such as solar, wind, and hydropower [1,2]. Renewable resources, which continue to grow in utilization, still have many sustainability challenges related to economics, efficiency, supplies, and storage [3]. Thus, continued efforts are needed to address these and other challenges when seeking to use renewable energy. One current area of exploration is the development of carbohydrate fuel cells that utilize biomass as the carbohydrate source [4–9]. Biomass sources for carbohydrate fuel cells have included various constituents of wood, alcohols, agricultural crops, biogas, and solid waste [10].

One key aspect of sustainable carbohydrate fuel cells is the need for sufficiently fast and efficient oxidation rates to enable the viable transfer of available electrons from the carbohydrate at current densities that will meet the power requirements for the application(s) of interest. In general, a C_n carbohydrate has a maximum $4n$ available electrons that can be extracted to produce energy. For example, the C_6 carbohydrate glucose ($C_6H_{12}O_6$) has 24 available electrons.

There are several types of carbohydrate fuel cells. One type is a biofuel cell utilizing carbohydrates in which either microbial catalysts (microbial fuel cell) or enzymatic catalysts (enzymatic biofuel cell) are employed. Biological catalysts provide advantages that include carbohydrate specificity and a reduction in byproducts. However, the use of biological catalysts faces potential challenges that include low power output, enzyme durability, transport limitations, and process limitations (e.g. pH) [11–14]. Carbohydrate fuel

* Corresponding author. 330S Engineering Building, Brigham Young University, Provo, UT, 84602, USA.
E-mail address: randy.lewis@byu.edu (R.S. Lewis).

https://doi.org/10.1016/j.renene.2019.07.079
0960-1481/

cells which use biological catalysts can extract up to 89% of available electrons in glucose but with a low power output which is not appropriate for large-scale systems [15,16].

A second type of carbohydrate fuel cell is one that does not utilize biological catalysts or any type of mediator. Rather precious metals such as platinum and gold are used as the anode which can result in rapid electron transfer rates and higher power densities [17,18]. However, this type of carbohydrate fuel cell has potential limitations including low electron transfer efficiencies, poisoning by chloride ions, and costly electrodes [19,20].

A third type of carbohydrate fuel cell, which is the focus of this study, utilizes an electron mediator. Electron mediators have been utilized to mitigate some of the challenges associated with biological catalysts. Viologen electron mediators have been shown to enhance electron transfer rates and improve carbohydrate conversion efficiencies [5,6]. In one study, the electron transfer rates of four different carbohydrates at two different temperatures in the presence of viologen electron mediators were measured. Based on the experimental rate constant of methyl viologen (the electron mediator) and glucose at 55 °C, a current density of 30 mA/cm^2 was estimated for a carbohydrate fuel cell [21]. In another study, it was shown that a high electron transfer efficiency was achieved at viologen/carbohydrate ratios greater than 10 and a simple mechanistic model was described [22]. In addition, it has been shown that the oxidation efficiency with use of viologen mediators was greater than 40% for some carbohydrates when measured with an O_2-uptake vial method [6]. Potential drawbacks to using electron mediators includes degradation, non-specific (e.g. complex) reactions leading to side products, and mediator retention.

Mediator retention is a key aspect in developing a sustainable carbohydrate fuel cell using electron mediators and possibilities exist to use polymers or moieties attached to the electrode surface to address retention issues. Several studies have shown a stable and good redox behavior of a viologen moiety in self-assembled monolayers of viologen derivatives on the electrode surface [23–26]. Also, viologen polymers have been shown to rapidly oxidize carbohydrates [27]. Although mediator retention has not been sufficiently studied, these studies suggest some potentially viable methods that could be further explored to address mediator retention.

Since the many types of carbohydrate fuel cells have many challenges but still show promising opportunities, mitigating the challenges necessitates the need to have a greater understanding of key aspects of the carbohydrate fuel cell process. With carbohydrate fuel cells using electron mediators, a two-step process occurs on the anode side. First, electrons are transferred from the carbohydrate to the electron mediator (homogeneous reaction in solution). Second, electrons are then transferred from the electron mediator to the electrode (heterogeneous reaction at electrode surface). Both steps are important to understand and characterize since the limiting step controls the rate of electron transport. The focus of this work is the characterization of the first step in which viologen is used as an electron mediator to accept electrons from the carbohydrate. Characterization of the first step, which was studied in the absence of a fuel cell to decouple the homogeneous kinetics from the heterogeneous kinetics, is essential for identifying process improvements that can enhance the overall electron transfer rate and the associated performance of a carbohydrate fuel cell.

Fig. 1 schematically shows the interaction of a viologen mediator, in this case methyl viologen (MV), with glucose as a representative C_n carbohydrate (n = 6) in the two-step electron transfer process. In the homogeneous first step, MV^{2+} (oxidized MV) in solution oxidizes the carbohydrate and, in the process, is reduced to MV^+ (reduced MV). The oxidation products may include carbonate

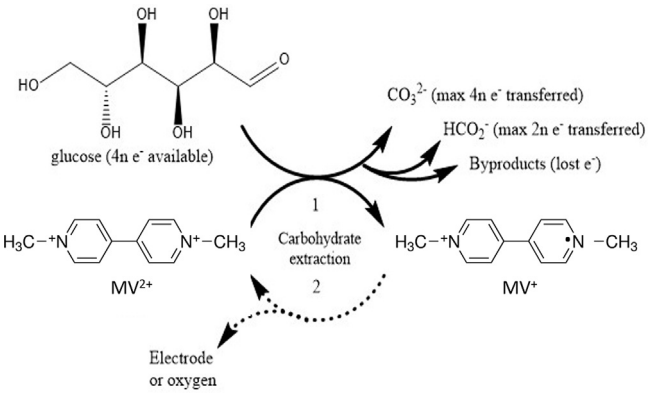

Fig. 1. The carbohydrate electron transfer process in the presence of methyl viologen (MV) and a representative C_n carbohydrate (C_6 glucose). The C_n carbohydrate has *4n* available electrons that can transfer completely to carbonate (CO_3^{2-}), partially to formate (HCO_2^-), or to other byproducts. In the first step, oxidized MV (MV^{2+}) is reduced by the carbohydrate to form reduced MV (MV^+). In the second step, reduced MV is re-oxidized at the electrode to form oxidized MV.

(CO_3^{2-}), which is the result of complete oxidation; formate (HCO_2^-), which is associated with release of half of the available electrons; or other byproducts, which corresponds to the release of a lower fraction of the carbohydrate energy. When a carbohydrate fuel cell is employed (which was not part of this study), the heterogeneous second step also occurs where the reduced MV^+ is then re-oxidized at the electrode to regenerate MV^{2+} while providing the anodic reaction for the fuel cell. Other viologens undergo a similar process.

According to an earlier study [21], the limiting step for a viologen-mediated carbohydrate fuel cell appears to be the homogeneous first step in which electrons are extracted from the carbohydrate to form MV^+. Thus, characterizing the kinetics of this first step is critical for obtaining kinetic-controlled parameters that can then be used to assess rate-controlling limitations when a carbohydrate fuel cell is employed. Although a simple mechanistic model was previously developed to characterize the homogeneous first step [21], a more rigorous model would provide additional information and more accurate assessment towards identifying the rate controlling step(s) that would limit the function of a carbohydrate fuel cell. In this work, the homogeneous first step using MV as the electron mediator was characterized with regards to pH, MV^{2+} concentration, carbohydrate concentration, and exposure time to buffer solutions when using glucose as a model carbohydrate.

2. Materials and methods

Two studies were performed to characterize the first step of the electron transfer process, which is the homogenous electron transfer rate between a carbohydrate and MV^{2+}. As previously stated, the first step was studied in the absence of a fuel cell to decouple the homogeneous kinetics from the heterogeneous kinetics. The first study measured the initial electron transfer rates between various carbohydrates and MV^{2+} in solution to provide a comparison of rates. The second study measured the initial electron transfer rate between glucose and MV^{2+} in solution to develop a rigorous mechanistic model for characterizing the homogeneous rate as a function of pH, MV^{2+} concentration, carbohydrate concentration, and exposure time to buffer solutions. For all studies, methyl viologen hydrate (MV^{2+}, 98% purity) was utilized. Six-carbon carbohydrates (glucose, fructose, mannose, galactose, and rhamnose), five-carbon carbohydrates (ribose, arabinose, and xylose), and the three-carbon carbohydrate dihydroxyacetone

(DHA) were evaluated in this study.

For the first study, the six-carbon, five-carbon, and three-carbon carbohydrates were equilibrated at pH 11 (0.50 M potassium phosphate buffer solution) for 5 min in a 3.5-ml cuvette under anaerobic conditions. An anaerobic MV^{2+} solution was then added to initiate the electron transfer from the carbohydrate to MV^{2+}. This study was performed at 50 °C with initial concentrations of 23.6 mM carbohydrate and 11.8 mM MV^{2+}.

For the second study, glucose was used as the model carbohydrate and all experiments were conducted at 50 °C. The influences of pH (11 and 12), carbohydrate concentration (1 and 2 mM), exposure time (0–100 min) to buffer, and initial MV^{2+} concentration (2, 4, 8, and 16 mM) on the electron transfer rate were examined. Separate stock solutions of glucose and MV^{2+} were prepared with deionized water, purged with nitrogen to remove oxygen, then placed in an incubator to preheat the solutions to 50 °C. Sodium hydroxide was added to a potassium phosphate solution to obtain the desired pH and was then purged with nitrogen to remove oxygen. The buffer was placed in 3.5-ml cuvettes in an oxygen-free glovebox and preheated in an incubator oven to 50 °C. The glucose stock solution was then added to the buffer solution by a gas-tight syringe to obtain the desired starting glucose concentration. Glucose remained in the buffer solution for incubation times ranging from 0 to 100 min. The MV^{2+} stock solution was then added with a gas tight syringe to initiate the electron transfer. After each run, the pH was measured to confirm that the pH remained constant during the experiment.

For all studies, absorbance was measured as a function of time at a wavelength of either 603 nm or 730 nm using a spectrophotometer with a heating block to maintain the desired temperature. Using the reported extinction coefficient of 13000 $M^{-1}cm^{-1}$ at 603 nm [28] or the measured extinction coefficient of $2737 \pm 42\ M^{-1}\ cm^{-1}$ at 730 nm, the initial slope of the absorbance versus time curve (observed during the first 2–3 min) was converted to the initial rate of MV^{+} formation ($r_{MV^+,i}$). Here, $r_{MV^+,i}$ also corresponds to the initial electron transfer rate. The use of varying wavelengths allowed for adjusting the sensitivity of the analysis.

3. Results

3.1. Electron transfer rates for various carbohydrates

For the first study, the value of $r_{MV^+,i}$ at pH 11 for the various carbohydrates is shown in Table 1 with $r_{MV^+,i}$ initially modeled as:

$$r_{MV^+,i} = k(C)_i(OH^-) \quad (1)$$

where $(C)_i$ is the initial concentration of the carbohydrate and k is the second-order rate constant. Table 1 also shows the calculated values of k for the various carbohydrates.

As noted, $r_{MV^+,i}$ (and the associated k values) generally increases as the number of carbons in the carbohydrates decreases. The values of $r_{MV^+,i}$ and k for ribose and DHA were difficult to assess since they occurred much more rapidly relative to the other carbohydrates-only lower bound estimates are provided. For the C_6 carbohydrates, fructose and galactose had $r_{MV^+,i}$ and k values of approximately 3–4 times higher than those of glucose, rhamnose, and mannose. A possible explanation for the faster fructose rate compared to glucose is provided later in the discussion.

Table 1
Rate constants for the Reaction of MV^{2+} with carbohydrates at pH 11 and 50 °C.

Carbohydrate	# of Carbons	$r_{MV^+,i}$(μM s^{-1})	k (M^{-1} s^{-1})
Mannose	6	1.01	0.043
Rhamnose	6	1.23	0.052
Glucose	6	1.39	0.059
Galactose	6	3.30	0.14
Fructose	6	4.72	0.20
Arabinose	5	3.54	0.15
Xylose	5	3.78	0.16
Ribose	5	14.2	>0.6
DHA	3	35.4	>1.5

3.2. Electron transfer rate between glucose and methyl viologen

The second set of experiments focused on glucose as the model carbohydrate to provide a more rigorous mechanistic characterization of $r_{MV^+,i}$ based on pH, MV^{2+} concentration, carbohydrate concentration, and exposure time to buffer. Fig. 2 shows the initial rate of MV^{+} formation, $r_{MV^+,i}$, at pH 12 in the presence of initial MV^{2+} concentrations varying from 2 to 16 mM. Here, glucose was incubated in buffer solution from 0 to 100 min prior to the reaction with MV^{2+}. The experiments showed good repeatability. As is evident, the glucose incubation time had a significant impact on $r_{MV^+,i}$, with an increasing rate with incubation time. The solid lines in Fig. 2 represent the rigorous model described in the discussion section. As seen, $r_{MV^+,i}$ appears to be slightly dependent on the MV^{2+} concentration at zero incubation time, particularly at 2 mM.

Fig. 3 shows $r_{MV^+,i}$ as a function of incubation time at (a) pH 11 and 12 and (b) glucose concentrations of 1 and 2 mM. The solid lines represent the rigorous model described in the discussion section. Based on Equation (1), the ratio of $r_{MV^+,i}$ at pH 11 relative to pH 12 at each time point should be (0.001M)/(0.01M) = 0.1 for the dependence of pH to be appropriately accounted for in Equation (1). For the three incubation time points evaluated at both pH values shown in Fig. 3a, the average ratio is 0.23 which is a little higher than this expectation. As shown, the strong pH effect is generally captured by both the model and the data even though the model slightly under predicts the effect. As for the effect of glucose on $r_{MV^+,i}$, the ratio of $r_{MV^+,i}$ at 1 mM glucose relative to 2 mM glucose at each time point should be (1 mM)/(2 mM) = 0.5 for the dependence of glucose to be appropriately accounted for in Equation (1). Fig. 3b shows an average ratio of 0.46 which is consistent with expectations. Thus, $r_{MV^+,i}$ has a first-order dependence on both pH and carbohydrate concentration.

Interestingly, the glucose exposure time to buffer prior to the reaction with MV^{2+} had a significant impact on $r_{MV^+,i}$. To further explore whether $r_{MV^+,i}$ of other carbohydrates are affected by the incubation time, fructose incubation was studied under the same

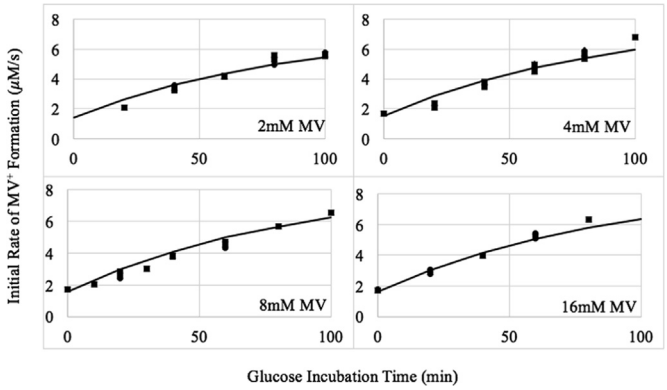

Fig. 2. Initial rate ($r_{MV^+,i}$) of reduced methyl viologen (MV^+) formation in the presence of 2 mM glucose versus glucose incubation time at pH 12 and 50 °C. Initial MV^{2+} concentrations were 2, 4, 8, and 16 mM. Previous to starting the reaction, the glucose was incubated in the buffer solution for various times ranging from 0 to 100 min. The symbols represent the data and the solid lines represent Equation (5).

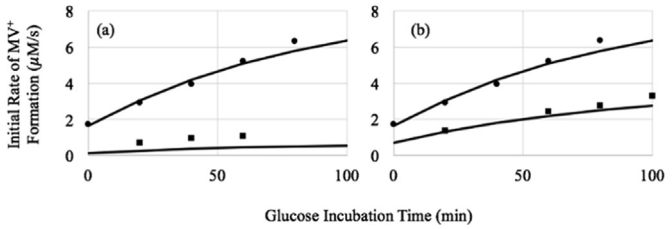

Fig. 3. Initial rate ($r_{MV^+,i}$) of reduced methyl viologen (MV^+) formation in the presence of 16 mM MV^{2+} versus glucose incubation time at 50 °C. Previous to the reaction, the glucose was incubated in the buffer solution for various times ranging from 0 to 100 min. (a) 2 mM glucose at pH 11 (squares) or pH 12 (circles). (b) pH 12 at 1 mM glucose (squares) or 2 mM glucose (circles). Solid lines represent Equation (5).

conditions as glucose incubation (pH 12 with an initial fructose concentration of 2 mM and an initial MV^{2+} concentration of 8 mM). As shown in Fig. 4, $r_{MV^+,i}$ decreased with incubation time when fructose was the starting carbohydrate, which is opposite to the increase observed for glucose. At an incubation time of zero, the value of $r_{MV^+,i}$ with fructose was much higher than that of glucose, similar to the findings in Table 1 at pH 11. Fig. 4 also shows the fit of the rigorous model for the glucose data. As discussed below, it appears that there is a conversion between glucose and fructose when the carbohydrate is exposed to a buffer solution and this conversion can account for the observed results. Further studies would need to be performed to assess incubation time effects on other carbohydrates.

4. Discussion

The values of $r_{MV^+,i}$ shown in Table 1, which represent the initial electron transfer rates between the carbohydrate and the viologen, provided insights into general trends of transferring electrons between carbohydrates and MV^{2+}. The electron transfer rates generally conform to the following trend for mono-carbohydrate oxidation by MV^{2+}: hexoses < pentoses < trioses. The carbohydrate experiments shown in Table 1 were first analyzed by a second-order rate law as shown by Equation (1). This rate model properly accounted for the effects of pH (hydroxide concentration) and carbohydrate concentration. However, the slight dependency on MV^{2+} concentration observed in the second study is not accounted for in Equation (1). In addition, the effect of the carbohydrate incubation time is not accounted for. When seeking to design a carbohydrate fuel cell, it is important to characterize electron transfer kinetic regimes in order to optimize the system. Thus, there is a need to develop a more rigorous electron transfer rate model to account for the incubation time as well as the potential effects of MV^{2+} concentration.

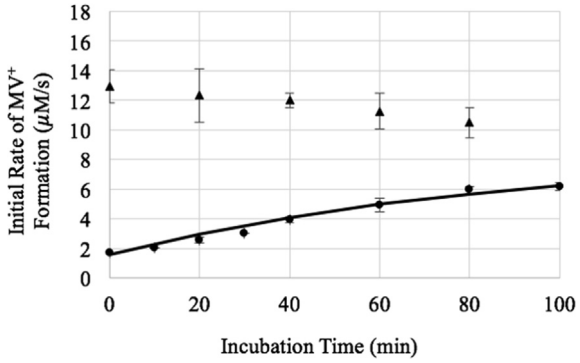

Fig. 4. The initial rate ($r_{MV^+,i}$) of reduced methyl viologen (MV^+) formation in the presence of 2 mM fructose and 8 mM MV^{2+} (triangles) or 2 mM glucose and 8 mM MV^{2+} (circles) versus incubation time at pH 12 and 50 °C. Previous to starting the reaction, the carbohydrate was incubated in the buffer solution for various times. The solid line represents Equation (5).

4.1. Reaction mechanism

Fig. 5 shows the proposed reaction mechanism developed by this study for electron transfer between a carbohydrate (glucose (G) and/or fructose (F) for this study) and MV^{2+}. The mechanism was developed using known carbohydrate chemistry along with the experimental information of this study. A key focus of the mechanism development was to reduce the complex carbohydrate chemistry to a simplified model while maintaining integrity between the model predictions and experimental data. The initial step of the mechanism shows that glucose (G) and fructose (F), upon reaction with the hydroxide ion, form rapid equilibrium species denoted as G′ and F′ as previously described in the literature [29]. MacLaurin and Green [30] studied the kinetics between a glucose, fructose, and mannose system and determined that the reaction path between the glucose and fructose is the fastest between those carbohydrates, confirming interconversion between F and G. In several studies, it was also determined that distinct enediolates form between F′ and G′ and via side pathways beginning with F′ and G'. As the enediolates are not very stable, they can form and react quickly [29–31]. Only through enediolate formation (denoted E_G and E_F) and subsequent reaction with MV^{2+} via side pathways with G′ and F′ was the mechanism consistent with the experimental results. Enediolate formation between G′ and F′ and subsequent reaction with MV^{2+} was not consistent with experimental results. Thus, no enediolates between G′ and F' are shown although they are known to exist. In addition, enediolate decomposition to other unknown species denoted as D_G and D_F was included, which is consistent with enediolate decomposition previously described [29].

4.2. Model for the initial rate of MV^+ formation ($r_{MV^+,i}$)

The following method and equations were used to obtain a more rigorous rate expression for $r_{MV^+,i}$ compared to Equation (1). First, based on Fig. 5, $r_{MV^+,i}$ was defined according to

$$r_{MV^+,i} = k_{MF}(E_F)\left(MV^{2+}\right) + k_{MG}(E_G)\left(MV^{2+}\right) \quad (2)$$

A pseudo-steady state hypothesis analysis was used to

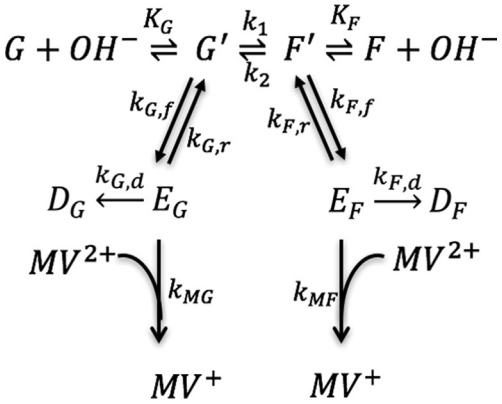

Fig. 5. Proposed reaction mechanism for glucose, fructose, and their enediolates with methyl viologen (MV^{2+}). G′ and F′ are equilibrium species, E represents an enediolate, and D represents a decomposition product.

approximate the concentrations of E_G and E_F since enediolates are at very low concentrations relative to other species due to rapid formation and depletion [30,31]. The rapid equilibrium assumptions of $G' = K_G(G)(OH^-)$ and $F' = K_F(F)(OH^-)$ and a pseudo-steady state assumption for E_G and E_F were applied to predict the approximate concentrations of E_G and E_F according to Equations (3) and (4), respectively.

$$E_G = \frac{k_{G,f}K_G(G)(OH^-)}{k_G' + k_{MG}\left(MV^{2+}\right)} \tag{3}$$

$$E_F = \frac{k_{F,f}K_F(F)(OH^-)}{k_F' + k_{MF}\left(MV^{2+}\right)} \tag{4}$$

Here, $k_G' = k_{G,r}+k_{G,d}$ and $k_F' = k_{F,r}+k_{F,d}$. For this study, it was assumed that $k_G' \approx k_{G,r}$ since decomposition products of glucose are relatively small [29]. It was also assumed that $k_F' \approx k_{F,r}$ is small over the incubation time studied since $r_{MV^+,i}$ increased with incubation time and significant degradation of fructose would lead to decreasing $r_{MV^+,i}$. These predictions were then substituted into Equation (2) to obtain $r_{MV^+,i}$ when glucose is initially present as shown in Equations (5) and (6).

$$r_{MV^+,i} = \frac{k_{G,f}K_G(G_0)(OH^-)\left(MV^{2+}\right)}{k_{G,ratio} + \left(MV^{2+}\right)} f \tag{5}$$

$$f = \left[1 + \left[\frac{k_{F,f}K_F\left[k_{G,ratio} + \left(MV^{2+}\right)\right]}{k_{G,f}K_G\left[k_{F,ratio} + \left(MV^{2+}\right)\right]} - 1\right]\frac{(F)}{(G_0)}\right] \tag{6}$$

Here, $k_{G,ratio} = k_G'/k_{MG}$, $k_{F,ratio} = k_F'/k_{MF}$, and (G_0) is the initial glucose concentration. Interestingly, the ratio (F)/(G_0) is present in Equation (6) and this ratio can change, especially during the incubation period where interconversion between fructose and glucose can occur. Thus, a method to estimate f from Equation (6) prior to the time MV^{2+} is added is required for parameterizing $r_{MV^+,i}$ based on the data. Clearly, if glucose did not convert to fructose during incubation, then $f = 1$ since (F)/(G_0) would be zero.

During glucose incubation in buffer in the absence of MV^{2+} (k_{MG} and k_{MF} are not applicable), Equations (7) and (8) describe the change in the total glucose concentration, $(G^T) = (G) + (G')$, and the total fructose concentration, $(F^T) = (F) + (F')$, with incubation time (t_i).

$$\frac{\partial G^T}{\partial t_i} = -\left(k_{G,f} + k_1\right)(G') + k_2(F') + k_{G,r}(E_G) \tag{7}$$

$$\frac{\partial F^T}{\partial t_i} = -\left(k_{F,f} + k_2\right)(F') + k_1(G') + k_{F,r}(E_F) \tag{8}$$

The rapid equilibrium assumptions of $(G^T) = (G)[1 + K_G(OH^-)]$ and $G' = K_G(G)(OH^-)$ for glucose and $(F^T) = (F)[1 + K_F(OH^-)]$ and $F' = K_F(F)(OH^-)$ for fructose are then substituted into Equations (7) and (8). In addition, Equations (3) and (4) (with $MV^{2+} = 0$) are also substituted to give the resulting Equations (9) and (10).

$$\frac{d(G)}{dt_i} = \frac{-k_1K_G(G)(OH^-) + k_2K_F(F)(OH^-)}{[1 + K_G(OH^-)]} \tag{9}$$

$$\frac{d(F)}{dt_i} = \frac{k_1K_G(G)(OH^-) - k_2K_F(F)(OH^-)}{[1 + K_F(OH^-)]} \tag{10}$$

Equations (9) and (10) thus characterize the interconversion between glucose and fructose during incubation in a buffer solution in the absence of MV^{2+}.

Equations (9) and (10) were solved to estimate (F)/(G_0) with t_i. At the initial time, only glucose was considered present since this represented the experimental procedure. Based on Equations 9 and 10, d(G) = -d(F). Thus, $(G) = (G_0) - (F)$. Substituting this relationship into Equation (10) and dividing both sides by (G_0) gives

$$\frac{d[(F)/(G_0)]}{dt} = a - b\,[(F)/(G_0)] \tag{11}$$

where

$$a = \frac{k_1K_G(OH^-)}{[1 + K_F(OH^-)]} \tag{12}$$

$$b = \frac{(k_1K_G + k_2K_F)(OH^-)}{[1 + K_F(OH^-)]} \tag{13}$$

Integration of Equation (11) gives $(F)/(G_0) = [(F)/(G_0)]_{ss}(1 - e^{-bt_i})$ where $[(F)/(G_0)]_{ss}$ is the steady state value of $[(F)/(G_0)]$ and is equivalent to a/b. To estimate a and b, and subsequently $[(F)/(G_0)]_{ss}$, values for k_1 and k_2 were obtained from literature at 50 °C and were 9.17×10^{-4} s^{-1} and 4.33×10^{-4} s^{-1}, respectively [29]. In addition, K_F and K_G were evaluated at 50 °C as 20.4 M^{-1} and 16.2 M^{-1}, respectively [29]. At pH 11, a and b are $1.45\ x\ 10^{-5}\ s^{-1}$ and $2.33\ x\ 10^{-5}\ s^{-1}$, respectively. At pH 12, a and b are $1.23\ x\ 10^{-4}\ s^{-1}$ and $2.0\ x\ 10^{-4}\ s^{-1}$, respectively. However, $[(F)/(G_0)]_{ss}$ is independent of pH and has a value of 0.62.

The above model for (F)/(G_0) along with the assumption that $[k_{G,ratio} + (MV^{2+})] = [k_{F,ratio} + (MV^{2+})]$ was substituted into Equation (6) to give f as a function t_i:

$$f = \left[1 + \left[\frac{k_{F,f}K_F}{k_{G,f}K_G} - 1\right]\left[\frac{(F)}{(G_0)}\right]_{ss}\left(1 - e^{-bt_i}\right)\right] \tag{14}$$

When fructose is initially present, similar equations to Equations (5) and (14) are obtained except all terms with F are changed to G and all terms with G are changed to F. Equation (5), with the definition of f in Equation (14), is the model used to characterize the electron transfer rate between glucose and MV^{2+}.

The value for $k_{F,f}$ relative to $k_{G,f}$ was determined from Equation (5) and Fig. 4 at $t_i = 0$ since $f = 1$. When $r_{MV^+,i}$ is independent of MV^{2+} then:

$$\frac{r_{MV^+,i\ (starting\ with\ F)}}{r_{MV^+,i\ (starting\ with\ G)}} = R = \frac{k_{F,f}K_F(F_0)}{k_{G,f}K_G(G_0)} \tag{15}$$

From Fig. 4 at $t_i = 0$, R is 7.7. Since F_0 and G_0 were equivalent, $k_{F,f} = 6.1\ k_{G,f}$ according to Equation (15). Therefore, the only remaining unknowns in Equations (5) and (14) are $k_{G,f}$ and $k_{G,ratio}$. All data in Fig. 2 were regressed to Equations (5) and (14) to obtain $k_{G,f} = 5.2 \times 10^{-3}$ s^{-1} and $k_{G,ratio} = 0.38$ mM. With the known ratio of $k_{F,f}$ to $k_{G,f}$, the value of $k_{F,f}$ was determined to be 3.1×10^{-2} s^{-1}. These values are all at 50 °C.

4.3. Data and model consistency

The data for $r_{MV^+,i}$ as a function of t_i, presented in Fig. 2, has a nearly linear trend. This can be explained by Equation (14) where the part of the model that is effected by incubation time is $(1 - e^{-bt_i})$. When b is small, $e^{-bt_i} \approx 1 - bt_i$. This is consistent for the values of b noted above. Therefore, $(1 - e^{-bt_i}) \approx bt_i$ which shows the model is consistent with the near linear trend of the experimental

data. Another consistency of Equation (14) with data is shown in Fig. 4 where $r_{MV^+,i}$ decreased with incubation time starting with fructose and $r_{MV^+,i}$ increased with incubation time starting with glucose. When starting with glucose, the $[k_{F,f}K_F/k_{G,f}K_G - 1]$ term is positive, leading to an increase in $r_{MV^+,i}$ with incubation time. However, when starting with fructose, the term becomes $[k_{G,f}K_F/k_{F,f}K_F - 1]$, which is negative, leading to a decrease in $r_{MV^+,i}$ with incubation time.

Fig. 6 shows the predicted initial rate data versus the experimental rate for all of the data. The line shows where each data point would lie if the experimental results and the model were in complete agreement. The solid lines in Figs. 2 and 3 also show the model fits for the experimental data. In general, the model did very well in capturing the dependence of MV^{2+} concentration, pH, carbohydrate concentration, and incubation time on $r_{MV^+,i}$. Generally, when the MV^{2+} concentration is $\gg k_{G,ratio}$ then the MV^{2+} dependence disappears. Thus, there is a first-order dependence on MV^{2+} concentration at very low concentrations and no dependence at higher concentrations when $MV^{2+} > 10k_{G,ratio}$ (around 3.8 mM for the carbohydrates in this study).

To compare with the carbohydrate studies shown in Table 1 at pH 11, which utilized an MV^{2+} concentration of 11.8 mM and an incubation time of 5 min, Equation (5) becomes $r_{MV^+,i} = (0.997)k_{G,f}K_G(G_0)(OH^-)$. By comparing this with Equation (1), the glucose k value in Table 1 is equivalent to $0.997k_{G,f}K_G$. Thus, with $K_G = 16.2$, the equivalent glucose $k_{G,f}$ for Table 1 would be 3.7×10^{-3} s^{-1}, which is generally consistent with the fitted parameter. However, it should be noted that the rigorously fitted $k_{G,f}$ came from a much larger set of experimental data over a wider range of experimental conditions.

4.4. Carbohydrate fuel cell applications

Characterization of the homogenous electron transfer rate (step 1 in Fig. 1) is important when seeking to optimize the design of a carbohydrate fuel cell, especially when this rate is limiting. For example, if glucose is the carbohydrate feedstock, one may want to allow glucose to incubate before feeding the solution into the carbohydrate fuel cell to increase $r_{MV^+,i}$ due to the formation of fructose. However, if fructose is the carbohydrate feedstock, incubation would be a disadvantage since $r_{MV^+,i}$ would decrease as a result of glucose formation. The model for $r_{MV^+,i}$ also provides insights into the effects of pH, MV^{2+} concentration, and incubation time that can be useful for design considerations.

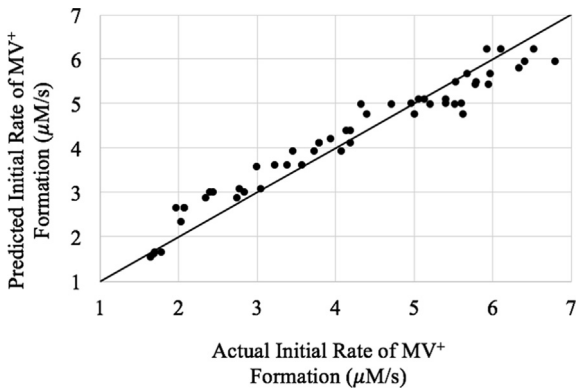

Fig. 6. Actual vs predicted initial rate ($r_{MV^+,i}$) of reduced methyl viologen (MV^+) formation of data in Fig. 2. The MV^{2+} concentration ranged from 2 to 16 mM and the incubation time ranged from 0 to 100 min. Each point represents an experimental data point and the line shows where each data point would lie if the experimental results and model were the same values.

To this point in the paper, the focus has been on the first step of the homogeneous electron transfer process in which the carbohydrate is oxidized and MV^{2+} is reduced to form MV^+. A detailed analysis of glucose as a model carbohydrate was performed, and appropriate rate expressions were developed. The intent, of course, is to use oxidation of a carbohydrate to generate electric power in a carbohydrate fuel cell. In the carbohydrate fuel cell, electron transfer at the anode occurs via the heterogeneous oxidation of MV^+, which regenerates MV^{2+} as shown in Step 2 of Fig. 1. This produces energetic electrons in the process according to:

$$MV^+ \rightarrow MV^{2+} + e^- \tag{16}$$

$$O_2 + 2H_2O + 4\,e^- \rightarrow 4\,OH^- \tag{17}$$

In a subsequent study that is currently in progress, a viologen-mediated fuel cell is being studied along with the development and validation of a detailed mathematical model to predict the performance of a viologen-mediated carbohydrate fuel cell. Here, unlike the study presented in this work, both the homogeneous reactions and the heterogeneous reactions are occurring simultaneously and are thus coupled. The developed rate expression in the present work is a crucial part of the mathematical model, especially since an earlier study suggested that the homogeneous electron transfer rate (Step 1) is limiting [21]. The mathematical model aims to predict the performance of a viologen-mediated carbohydrate fuel cell in terms of current/power density at various operating conditions for maximizing the performance. Results of the model, with validation via experiments, will be compared with current and power densities of other types of carbohydrate fuel cells reported in the literature [32–35].

5. Conclusions

This work focused on assessing and characterizing the homogeneous electron transfer rate between a carbohydrate and MV electron mediator, which is the first step in a carbohydrate fuel cell using MV as the mediator. Values for $r_{MV^+,i}$ (and the associated k values) for various monosaccharides were reported. The value of $r_{MV^+,i}$ generally increased as the number of carbons in the carbohydrates decreased. Using glucose as the model carbohydrate, a rigorous model was developed to show the dependence of MV^{2+} concentration, pH, carbohydrate concentration, and incubation time on $r_{MV^+,i}$. Model predictions agreed very well with experimental data. The effects of incubation time for a glucose system were consistent with interconversion between glucose and fructose. The OH^- concentration dependence was first order; thus, a pH change from 11 to 12 would result in a 10-fold increase in the reaction rate. Similarly, the glucose dependence was first order. The effect that the concentration of MV^{2+} has on $r_{MV^+,i}$ is a bit more complicated. There is MV^{2+} dependence at lower concentrations; however, as the concentration of MV^{2+} increases (to values about 10-fold larger than the $k_{G,ratio}$, or 3.8 mM), $r_{MV^+,i}$ is no longer dependent on the MV^{2+} concentration. The model for $r_{MV^+,i}$ also provides insights such as the effect of pH, MV^{2+} concentration, and incubation time that can be useful for carbohydrate fuel cell design consideration.

Acknowledgments

The authors acknowledge support by the National Science Foundation [NSF CBET-1540537]. The authors also appreciate editorial comments from Amir Sina Hamedi.

Appendix A. Supplementary data

Supplementary data to this article can be found online at

https://doi.org/10.1016/j.renene.2019.07.079.

References

[1] A. Hepbasli, A key review on exergetic analysis and assessment of renewable energy resources for a sustainable future, Renew. Sustain. Energy Rev. 12 (3) (2008) 593–661.

[2] U.S. Energy Information Administration, U.S. Energy Facts Explained. https://www.eia.gov/energyexplained/index.cfm?page=us_energy_home. (Accessed 14 February 2018).

[3] A. Angelis-Dimakis, M. Biberacher, J. Dominguez, G. Fiorese, S. Gadocha, E. Gnansounou, G. Guariso, A. Kartalidis, L. Panichelli, I. Pinedo, M. Robba, Methods and tools to evaluate the availability of renewable energy sources, Renew. Sustain. Energy Rev. 15 (2) (2011) 1182–1200.

[4] J. Xuan, M.K.H. Leung, D.Y.C. Leung, M. Ni, A review of biomass-derived fuel processors for fuel cell systems, Renew. Sustain. Energy Rev. 13 (6–7) (2009) 1301–1313.

[5] G. Watt, A new future for carbohydrate fuel cells, Renew. Energy 72 (2014) 99–104.

[6] D. Wheeler, J. Nichols, D. Hansen, M. Andrus, S. Choi, G.D. Watt, Viologen catalysts for a direct carbohydrate fuel cell, J. Electrochem. Soc. 156 (10) (2009) B1201–B1207.

[7] W. Liu, W. Mu, Y. Deng, High-performance liquid-catalyst fuel cell for direct biomass-into-electricity conversion, Angew. Chem. Int. Ed. 53 (49) (2014) 13558–13562.

[8] M. Hao, X. Liu, M. Feng, P. Zhang, G. Wang, Generating power from cellulose in an alkaline fuel cell enhanced by methyl viologen as an electron-transfer catalyst, J. Power Sources 251 (4) (2014) 222–228.

[9] Y. Yang, X. Liu, M. Hao, P. Zhang, Performance of a low-cost direct glucose fuel cell with an anion-exchange membrane, Int. J. Hydrogen Energy 40 (34) (2015) 10979–10984.

[10] U.S. Energy Information Administration, What is renewable energy?. https://www.eia.gov/energyexplained/index.cfm?page=renewable_home. (Accessed 28 February 2018).

[11] A.T. Yahiro, S.M. Lee, D.O. Kimble, Bioelectrochemistry: I. Enzyme utilizing bio-fuel cell studies, Biochim. Biophys. Acta (BBA) - Spec. Sect. Biophys. Subj. 88 (2) (1964) 375–383.

[12] R.A. Bullen, T.C. Arnot, J.B. Lakeman, F.C. Walsh, Biofuel cells and their development, Biosens. Bioelectron. 21 (11) (2006) 2015–2045.

[13] S. Park, H. Boo, T.D. Chung, Electrochemical non-enzymatic glucose sensors, Anal. Chim. Acta 556 (1) (2006) 46–57.

[14] F. Davis, S.P. Higson, Biofuel cells—recent advances and applications, Biosens. Bioelectron. 22 (7) (2007) 1224–1235.

[15] S.K. Chaudhuri, D.R. Lovley, Electricity generation by direct oxidation of glucose in mediatorless microbial fuel cells, Nat. Biotechnol. 21 (10) (2003) 1229.

[16] K. Rabaey, G. Lissens, S.D. Siciliano, W. Verstraete, A microbial fuel cell capable of converting glucose to electricity at high rate and efficiency, Biotechnol. Lett. 25 (18) (2003) 1531–1535.

[17] A. Brouzgou, P. Tsiakaras, Electrocatalysts for glucose electrooxidation reaction: a review, Top. Catal. 58 (18–20) (2015) 1311–1327.

[18] W. Liu, W. Mu, Y. Deng, High-performance liquid-catalyst fuel cell for direct biomass-into-electricity conversion, Angew. Chem. 126 (49) (2014) 13776–13780.

[19] K.E. Toghill, R.G. Compton, Electrochemical non-enzymatic glucose sensors: a perspective and an evaluation, Int. J. Electrochem. Sci 5 (9) (2010) 1246–1301.

[20] J. McGinley, F.N. McHale, P. Hughes, C.N. Reid, A.P. McHale, Production of electrical energy from carbohydrates using a transition metal-catalysed liquid alkaline fuel cell, Biotechnol. Lett. 26 (23) (2004) 1771–1776.

[21] G. Watt, Kinetic evaluation of the viologen-catalyzed carbohydrate oxidation reaction for fuel cell application, Renew. Energy 63 (2014) 370–375.

[22] G. Watt, D. Hansen, D. Dodson, M. Andrus, D. Wheeler, Electrical energy from carbohydrate oxidation during viologen-catalyzed O-2-oxidation: mechanistic insights, Renew. Energy 36 (5) (2011) 1523–1528.

[23] H.C. De Long, D.A.J.L. Buttry, Ionic interactions play a major role in determining the electrochemical behavior of self-assembling viologen monolayers, Langmuir 6 (7) (1990) 1319–1322.

[24] H.C. De Long, D.A.J.L. Buttry, Environmental effects on redox potentials of viologen groups embedded in electroactive self-assembled monolayers, Langmuir 8 (10) (1992) 2491–2496.

[25] N. Hosoda, H. Ohno, E.J.P. Tsuchida, Mediated electron transfer reactions at electrodes coated with poly(viologen)s, Polymer 25 (9) (1984) 1302–1306.

[26] J.Y. Ock, H.K. Shin, D.J. Qian, J. Miyake, Y.S. Kwon, Determining the self-assembling and redox process of a viologen monolayer by electrochemical quartz crystal microbalance, Jpn. J. Appl. Phys. 43 (4S) (2004) 2376.

[27] C.R. Rigby, H. Han, P.K. Bhowmik, M. Bahari, A. Chang, J.N. Harb, R.S. Lewis, G.D. Watt, Soluble viologen polymers as carbohydrate oxidation catalysts for alkaline carbohydrate fuel cells, J. Electroanal. Chem. 823 (2018) 416–421.

[28] R.N.F. Thorneley, A convenient electrochemical preparation of reduced methyl viologenand a kinetic study of the reaction with oxygen using an anaerobic stopped-flow apparatus, Biochim. Biophys. Acta Bioenerg. 333 (1974) 487–496.

[29] T. Vuorinen, E. Sjostrom, Kinetics of alkali-catalyzed isomerization of D-glucose and D-fructose in ethanol-water solutions, Carbohydr. Res. 108 (1) (1982) 23–29.

[30] D. Maclaurin, J. Green, Carbohydrates in alkaline systems .I. Kinetics of transformation and degradation of D-glucose,D-fructose, and D-mannose in 1 M sodium hydroxide at 22 Degrees C, Can. J. Chem. 47 (21) (1969) 3947–3955.

[31] L. Anderson, S. Wittkopp, C. Painter, J. Liegel, R. Schreiner, J. Bell, B. Shakhashiri, What is happening when the blue bottle bleaches: an investigation of the methylene blue-catalyzed air oxidation of glucose, J. Chem. Educ. 89 (11) (2012) 1425–1431.

[32] X. Liu, M. Hao, M. Feng, L. Zhang, Y. Zhao, X. Du, G. Wang, A One-compartment direct glucose alkaline fuel cell with methyl viologen as electron mediator, Appl. Energy 106 (2013) 176–183.

[33] D. Scott, T. Tsang, L. Chetty, S. Aloi, B. Liaw, Mechanistic understanding of monosaccharide-air flow battery electrochemistry, J. Power Sources 196 (24) (2011) 10556–10562.

[34] Z. Li, X. Liu, P. Liu, P. Zhang, The performance of electron-mediator modified activated carbon as anode for direct glucose alkaline fuel cell, Catalysts 6 (7) (2016) 95–106.

[35] X. Liu, Z. Li, Y. Yang, P. Liu, P. Zhang, Electricity generation from a refuelable glucose alkaline fuel cell with a methyl viologen-immobilized activated carbon anode, Electrochim. Acta 222 (2016), 1430-143.